# Effect of feed sprue size on porosity defects in Platinum 950 centrifugal investment casting via numerical modelling

# Effect of feed sprue size on porosity defects in Platinum 950 centrifugal investment casting via numerical modelling

**K. Munpakdee[1], P. Ninpetch[1], S. Otarawanna[2], R. Canyook[3], and P. Kowitwarangkul[1*]**

[1]The Sirindhorn International Thai-German Graduate School of Engineering, King Mongkut's University of Technology North Bangkok, Bangkok 10800, Thailand
[2]National Metal and Materials Technology Center (MTEC), National Science and Technology Development Agency (NSTDA), Pathum Thani 12120, Thailand
[3]Faculty of Engineering, King Mongkut's University of Technology North Bangkok, Bangkok 10800, Thailand

* Corresponding Author: pruet.k@tggs.kmutnb.ac.th

**Abstract**
The centrifugal investment casting process is typically used in the jewelry manufacturing industry. However, porosity defects are often found in jewelry castings made by this process. Porosity on the casting surface is a major concern for jewelry manufacturers as the defect leads to significant yield losses during the repair work. Improper feed sprue design is one of the major causes of porosity defects. The purpose of this work is to study the effect of feed sprue size on porosity defects in Platinum 950 jewelry made by the centrifugal investment casting process. Two feed sprue sizes were experimented in this study. FLOW-3D CAST software was employed for the casting process simulation. Simulation results were analysed together with experimental results quantified by an image analysis technique. The results show that the larger feed sprue provides castings with less porosity compared to the smaller feed sprue.

**Keywords:** Investment casting, Porosity, Platinum 950, Solidification, Computer simulation

## 1. Introduction

In the jewelry industry, centrifugal investment casting of precious metals such as platinum and gold, is a casting process providing the excellent finish surface and dimensions. However, only some castings are completely free of defects as this casting process has many variables that is difficult to control [1], e.g., casting temperature, flask temperature, centrifugal speed and casting atmosphere [2, 3]. Unsuitable process conditions lead to defects, such as porosity, in jewelry pieces. Porosity on the casting surface is one of major concerns for jewelry manufacturers. When it appears on the finish surface, it needs to be fixed. This results in the loss of productivity time and yield loss of raw materials.

Shrinkage porosity forms during solidification in the solidified part of specimen that lack of feeding to compensate the reduction in volume of the liquid-to-solid phase transition during the dendritic growth [4, 5]. In casting, the solidification can be divided into 2 types: directional solidification and progressive solidification [6]. During directional solidification, the molten metal starts to solidify from a smaller

modulus to a larger modulus [7]. For the progressive solidification, the molten metal solidifies from the casting surface to the casting center. When the progressive solidification dominates over the directional solidification, shrinkage porosity is likely to form [8].

In addition, the use of high superheat can enhance the fluidity during mold filling. However, it also causes the shrinkage porosity due to the volume expansion and contraction of the liquid as the consequence of the density change at high temperature [6]. To reduce the shrinkage porosity defects, proper feed sprues and component design which provides directional solidification and sufficient superheat of pouring temperature were commonly applied [6, 9-11].

Computer simulation technique is an effective method to solve the shrinkage porosity problem [12]. Over the past decade, the numerical modelling for centrifugal investment casting process has been developed to investigate and predict the effect of parameters in casting process [2, 13]. For instance, Fischer-Bühner J [14] studied casting defects of 18K gold alloys by using numerical simulation. They concluded that the different thermal properties of 18K gold alloys give rise to different sensitivity to shrinkage porosity. Chan et al. [15] investigated the influence of feed sprue design on the porosity of dental parts in investment casting process. It was found that the single main sprue design is less effective than double-sprue design to reduce internal porosity.

The aims of this research are to investigate the effect of feed sprue designs on porosity defects in jewelry casting by using numerical modelling. The material used in the study is Pt950Ru (95%Platinum - 5% Ruthenium), which is commonly used by jewelry manufacturers for high-end products [16]. The numerical simulation was performed by the commercial software "FLOW-3D CAST". This software is based on the Finite Volume Method (FVM) and Volume of fluid (VOF), which are commonly used to track the free surface of fluid flow during casting process [17]. Furthermore, image analysis technique was used to analyzed the simulation results and quantified experimental results

## 2. Methodology

The work in this study is divided into two parts: the first part is the numerical simulation which carried out by using commercial simulation software package FLOW-3D CAST Ver. 5.0 to perform 3D model simulation. In the second part, the experimental study was carried out to study the effect of pouring temperature and feed sprue design on porosity at Christy Gem Co., Ltd.

### *2.1 Process parameters and porosity characterization*

The study was conducted by simulation and experiments. The casting experiments were carried out by using Yasui, Vacuum Casting Machine 2014. The investment mold with flask is rotated around the vertical axis, Z and is simultaneously driven by centrifugal force [18]. The main process parameters used in this study include pouring temperature of 1,980$^{o}$C, flask temperature of 850$^{o}$C and ladle temperature of 600$^{o}$C obtained from Christy Gems Ltd. For porosity characteristic method, the specimens were ground and polished to analyze the cross-section area by image analysis in the experiment.

### *2.2 Mathematical Models of Numerical Simulation*

In the simulation, the governing equations of fluid dynamic consist of three equations: (1) mass conservation, (2) momentum conservation and (3) energy conservation respectively [19, 20]. In addition, turbulent modeling (k-ω) and volume of fluid (VOF) are used to solve turbulence flow of molten metal in the casting mold [17, 21].

$$\nabla \cdot \vec{V} = 0 \tag{1}$$

$$\frac{\partial \vec{V}}{\partial t} + (\vec{V} \cdot \nabla)\vec{V} = -\frac{1}{\rho}\nabla p + \nu \nabla^2 \vec{V} + \vec{f} \tag{2}$$

$$\rho c_p \left[\frac{\partial T}{\partial t} + (\vec{V} \cdot \nabla)T\right] = \lambda \nabla^2 T + \emptyset \tag{3}$$

where ρ and $\vec{V}$ are density and velocity vector, p is the pressure, ν is the kinematic viscosity, $\vec{f}$ is the body force per unit mass, $c_p$ is the specific heat at constant pressure, T is temperature, λ is thermal conductivity and ∅ is the dissipation function.

*2.3 CFD simulation setup and thermal-physical properties*

The 3D CAD model in this study comprises of ladle, mold, and casting tree. Four different feed sprue designs of the casting tree are shown in Figure 1(a). This paper primarily focuses on the results of the feed sprue design 1 (smaller feed sprue) and design 2 (larger feed sprue). The computational mesh of 9.6 million elements, with the mesh sizes ranging from 0.7 and 0.35 mm was used for the simulation. The 3D model is divided into 4 multi-mesh blocks with different mesh resolution as shown in Figure 1(b).

Furthermore, the probes were located at five positions of the ring to measure the temperature change of metal as illustrated in Figure 1(c). The gradient between probes P1 and P3 are used for the analysis of the shrinkage porosity in this study. Additionally, the material and thermophysical properties of Pt950Ru including solidus temperature (1,780°C), liquidus temperature (1,795°C), latent heat of fusion (122,000 J/kg), specific heat, density, thermal conductivity, and viscosity [2, 22, 23] were applied to the simulation setup.

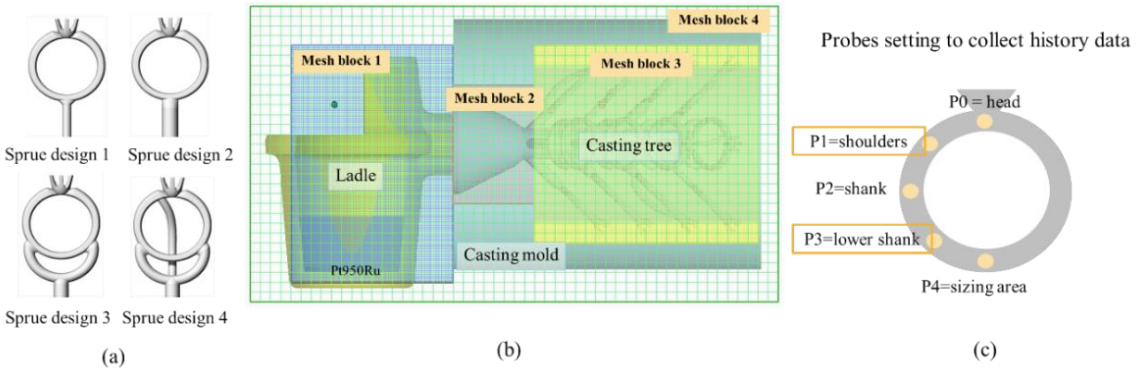


**Figure 1.** (a) The four different feeder sprue designs, (b) The assembling of 3D model casting tree with multi-mesh blocks with different mesh resolution, (c) schematic of probes setting in computer simulation.

## 3. Results and Discussion

The simulation results of casting at the pouring temperature of 1980°C from filling and solidification process were analyzed in this study. The molten metal filling process was done within 1 second and then the solidification started to simulate. The metal temperature was dropped from pouring temperatures to lower than liquidus temperature (1795°C) during the casting as shown in Figure 2. The color map showed the sequence of temperature variable in casting simulation process. The red and the blue color represented the initial pouring temperature and the solidus temperature at 1780°C. It could be seen that the larger feed sprue was filled sooner than small feed sprue because the diameter was bigger. The solidification results obtained from the simulation were further used to identify areas that could cause shrinkage porosity.

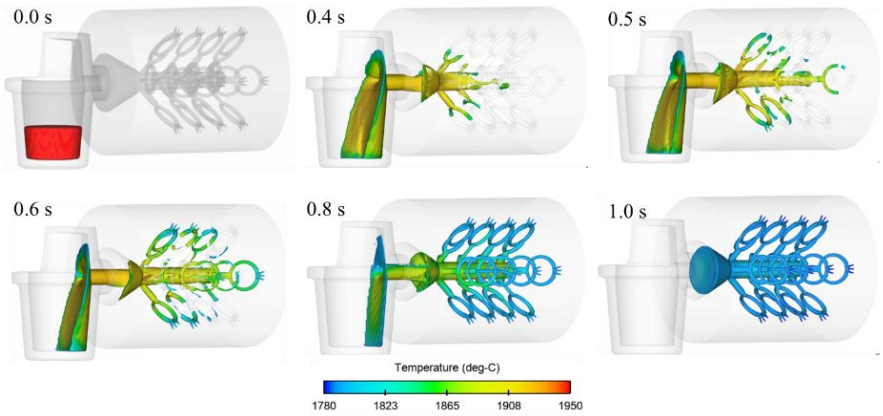


**Figure 2.** The temperature profile of filling and solidification process.

*3.1 The effects of feed sprue designs on the directional solidification behaviour and thermal gradient*

The shrinkage formation in solidification processes could be investigated and evaluated via the volume function through the color region. The 100% liquid metal and the solidified metal were indicated by red and grey colors. Figure 3 presented the fluid fraction of molten metal in the ring at the pouring temperature of 1980°C.

From the simulation results, it could be seen that when the casting time reaches at 1.8 and 1.9 seconds, the liquid metal in the ring with the smaller feed sprue started early in the stage of solidification. At 2.0 seconds, the liquid in the smaller feed sprue was completely solidified and blocks the feeding supply. Due to the lack of feeding supply for volume contraction during the growth of dendrite in solidification process, the smaller feed sprue with lower modulus volume could cause more shrinkage porosity formation. In contrast, the larger feed sprue with higher modulus volume that contained high temperature for a longer period of time could retard the heat transfer and cooling rate to allow more feeding supply for volume contraction. This process led to less formation of shrinkage porosity.

Moreover, the sequence of solidification of the ring with the larger feed sprue was more directional solidification which started from the head, shoulder, shank of ring compared to the ring with the smaller feed sprue. These results showed that the sprue designs had a significant effect on the directional solidification behavior and shrinkage porosity in jewelry casting.

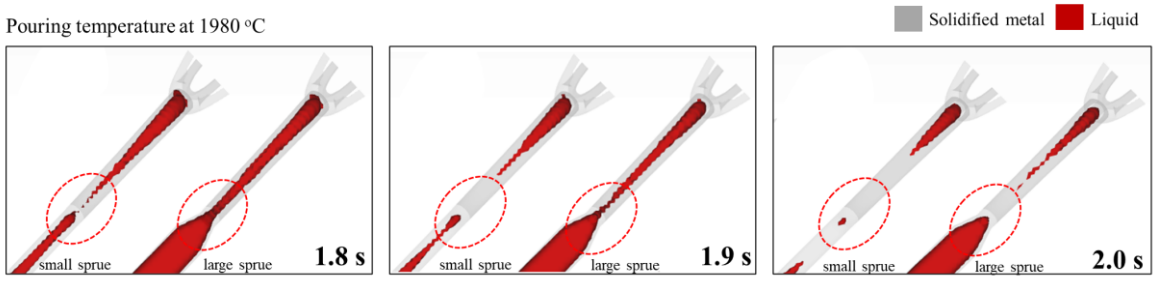


**Figure 3.** The fluid fraction of molten metal in the ring at pouring temperature at 1980°C

One of the quantitative indicators used in this study to indicate the directional solidification behavior was the solidification sequence that could be described by the thermal gradient between shoulder and shank of the ring. As described in the previous section, the probes P0-P4 were located on the ring to collect the change of temperature in casting process. Figure 4(a) and (b) illustrated the temperature change of probes P1 and P3 from the computer simulation with pouring temperature of 1980°C of the ring with smaller feed sprue and larger feed sprue. The dashed line represented the temperature change of P1 which was located in the shoulder area of the ring. The solid line represented the temperature change of P3 which was located in the lower shank area of the ring. In this study, the author observed

the average of thermal gradient which was calculated from three temperature reference points of P3 including 1793°C, 1788°C and 1783°C. The higher average thermal gradient or more positive value of P1 minus P3 was, the more opportunity of shrinkage formation was.

The simulation results showed that the ring with the larger feed sprue had the average thermal gradient value of 1.9°C due to slow heat loss during the solidification in feed sprue compared to the other conditions. On the other hand, the ring with the smaller feed sprue had the average thermal gradient value of 2.8°C as illustrated in Figure 5(a). When the temperature of P1 was higher than P3, the progressive solidification at shank area tended to be more dominant compared to the directional solidification which led to lack of liquid supply and less directional solidification sequence from shoulder to shank of the ring. Figure 5(a). showed the thermal gradient of each ring which was calculated from variable temperature of P1 and P3. Moreover, Figure 5(b) showed the results of different of temperature change in the ring between P1 minus P3. The result of the smaller feed sprue presented higher difference of temperature between P1 minus P3 due to less modulus and faster temperature change in feed sprue.

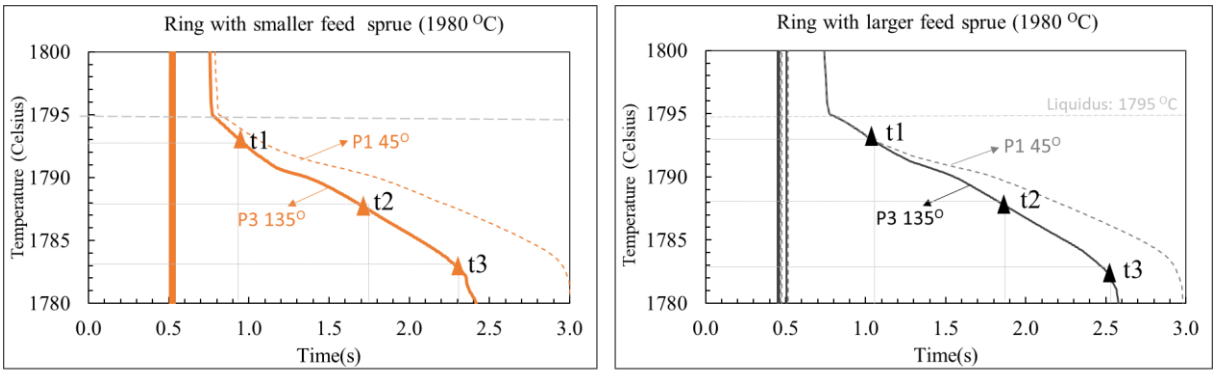


(a) (b)

**Figure 4.** Temperature change at probe P1 and P3 of the simulation at pouring temperature 1980 °C (a) smaller feed sprue, (b) larger feed sprue

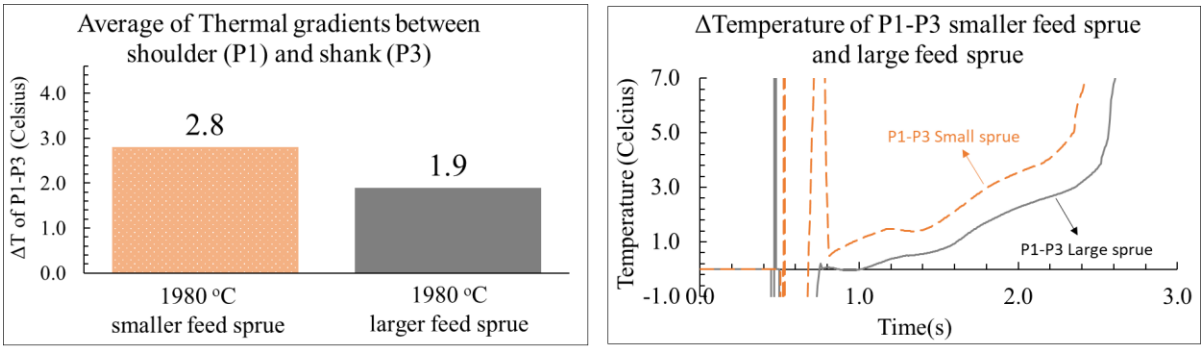


(a) (b)

**Figure 5.** (a) Average of thermal gradient of P1 minus P3 in the rings, (b) The temperature difference of P1 minus P3 in the rings.

*3.2 Experiment results with image analysis*

The cross section of the casting specimen from experiment were observed in this study by using the image analysis tools, optical microscope (OM) and "ImageJ" software. The total shrinkage porosity was indicated in percentage (%) compared to total area. Figure 6(a). shows the casting tree from the experiment with pouring temperature at of 1980°C. The porosity in cross section specimens can be found by the OM. To quantitatively analysis, ImageJ were used to count and calculate the total area of porosity on cross section area of specimen. As shown in Figure 6(b) the cross section of the ring with smaller

sprue has porosity for approximately 0.84% compared to the total area and the cross section of the ring with larger sprue has porosity for approximately 0.0015%.

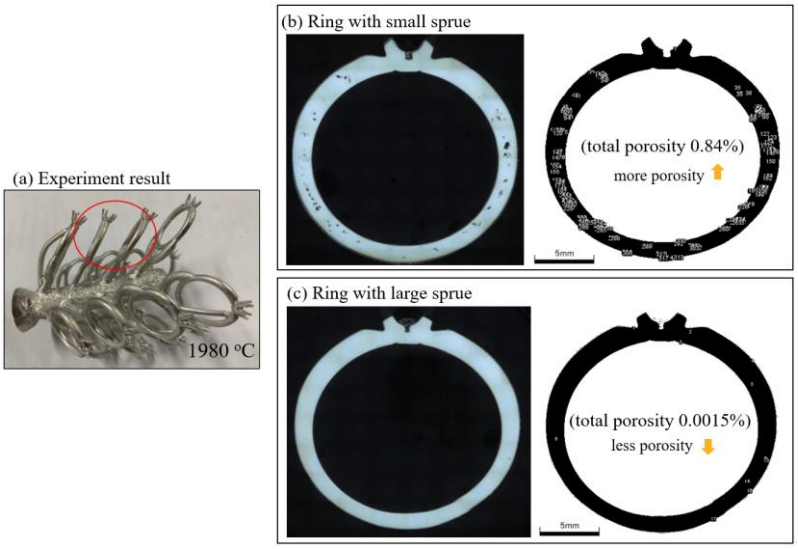


**Figure 6.** (a) The casting tree from experiment at pouring temperature of 1980°C, (b) Cross sectional ring with smaller sprue, (c) Cross sectional ring with larger sprue.

## 4. Conclusion

In this research, the numerical simulation and the experimental study were carried out to investigate the effect of feed sprue size on shrinkage porosity.

The simulation results show that the larger feed sprue provides a better result of the lowest average thermal gradient value of 1.9°C compared to the smaller feed sprue which has the highest average thermal gradient value of 2.8°C. The fluid fraction results reveal that feeding supply of molten metal in the larger feed sprue retards the temperature in the lower shank to prevent early solidification, while the molten metal solidified too early in the smaller feed sprue thus, it cannot compensate the volume contraction during the solidification.

In addition, the experimental results at the pouring temperature of 1980°C show that the total area of porosity on cross section of the ring with smaller feed sprue is 0.84%, while the porosity area of the ring with larger sprue is 0.0015%. The results indicate that the smaller feed sprue has the porosity more than the larger feed sprue.

## Acknowledgments

The authors gratefully thank Christy Gem Co., Ltd. for corporation and support. This research was funded by the Thailand Science Research and Innovation (TSRI) and National Research Council of Thailand (NRCT) contract no. RDG62T0036.

## References

[1] Dieter O 1998 *Handbook on Casting and Other Defects in Gold Jewelry Manufacture* (London: World Gold Council)
[2] Duncan M Tauriq K Penny P R Victoria H Ali B Irshad K and Candy L 2005 *Platinum Met.* Rev. **49**(4) 174-182
[3] Ulrich E K Tiziana H Dario T and Franz H 2015 *Jewelry Technology Forum* 2-10
[4] Silva F S 2010 *Proc. of 21st Santa Fe Symposium on Jewelry Manufacturing Technology* (New Mexico, USA)
[5] Pequet C Rappaz M and Gremaud M 2002 *Metal Mater Trans A.* **33**(7) 2095-2106

[6] Stefanescu D M 2008 *Science and Engineering of Casting Solidification, 2nd ed* (Berlin: Springer) 67
[7] Mark J 2005 *JOM.* **57**(5) 19-28
[8] Chastain S 2004 *Metal casting: a sand casting manual for the small foundry* (Jacksonville: Chastain Publishing)
[9] Dieter O 1997 *Gold Bulletin* **30**(1) 13-19
[10] Corti C and Holliday R 2010 Jewelry manufacturing technology Gold: Science and applications, (Boca Raton, FL: CRC Press)
[11] Eddie B 2002 *Gold Technol* **36** 3-11
[12] Mochamad A Poppy P Latief S and Yusuf A W 2020 *AIP Conf. Proc.* **2228** 030010-1- 030010-5
[13] Arblaster J W 2005 *Platinum Met. Rev.* **49**(3) 141-149
[14] Fischer-Bühner J 2007 *Proc. of 21st Santa Fe Symposium on Jewelry Manufacturing Technology* (New Mexico, USA)
[15] Daniel Ch Villa G Ronald B and Kwok-hung C 1997 *J. Prosthet. Dent*. **78**(4) 400-404
[16] Duncan M Tauriq K Penny P R Victoria H and Candy L 2005 *Platinum Met. Rev.* **49**(3) 110-117
[17] Tiziana H and Ulrich E K 2015 *Johnson Matthey Tech* **59**(2) 95-108
[18] Creeger G A 1994 Combination of Investment and Centrifugal Casting, *https://www.science.gov/topicpages/c/centrifugal+casting+technique.html*, accessed 1 May 2020
[19] Xuan-xuan Y Ling Ch and Yi-jie H 2012 *Energy Procedia* **17** 1864-1871
[20] Cüneyt S 2019 *Finite Element Analysis in Thermofluids* (Ankara: Middle East Technical University) 1-13
[21] Wilcox D C 2008 *AIAA Journal*. **46** 2823-2838
[22] Kent C and Christoph B 2008 *Proc. of 62nd SFSA Technical and Operating Conference* (Chicago, USA)
[23] Paul-François P 2014 *Johnson Matthey Tech* **58**(3) 124-136